SUPPORTING INFORMATION

N-terminal alternative splicing of GluN1 regulates the maturation of excitatory synapses and seizure susceptibility

Hong Liu, Hao Wang, Matthew Peterson, Wen Zhang, Guoqiang Hou, Zhong-wei Zhang*

Email: zhongwei.zhang@jax.org

This PDF file includes:

Materials and Methods

Figures. S1 to S8

www.pnas.org/cgi/doi/10.1073/pnas.1905721116

Materials and Methods

Animals. Mice were housed in the Research Animal Facility of The Jackson Laboratory. All animal procedures are in accordance with the NIH *Guide for the Care and Use of Laboratory Animals*, and have been approved by the Institutional Animal Care and Use Committee of The Jackson Laboratory.

Mice with deletion of *Grin2a* (*Grin2a*-KO), B6;129S-*Grin2a*^{tm1Nak} (1) were obtained from RIKEN RBC (Tsukuba Ibaraki, Japan). The *Grin2a*-KO strain has been backcrossed to C57BL/6J for over 10 generations. Genotypes were determined by PCR using three primers: 5'-CCAGAATCCTAAAGGCACAACC-3', 5'-AGTCACCCCTGTTGAGGATAGC-3', 5'-CGTCACCTTAATATGCGAAGT-3', which generate 203- and 360-bp products for the wild type (WT) allele and mutated allele, respectively. The genotyping protocol has been validated by quantitative RT-PCR and western blot using brain tissues from adult mice.

Generation of the Grin1*ΔEx5 *allele. Mice with *Grin1* exon 5 deletion (*Grin1*ΔEx5) were generated through targeted mutation in ES cells using standard procedures. Briefly, a BAC (RP23-360A18) from C57BL/6J (B6) containing the entire genomic region of *Grin1* was obtained from The Jackson Laboratory Molecular Biology Services and validated by BAC end sequencing. The targeting vector was generated by BAC recombineering. The first *loxP* site was inserted into the intron upstream of exon 5 of *Grin1*. The second *loxP* site together with the *frt*-PGK-NEO-*frt* selection cassette was inserted downstream of exon 5 of *Grin1*. The targeting vector also has a MC1-TK selection cassette after the 3' homology arm. Targeting was done in B6J ES cells and confirmed by long PCR and southern blot. Correctly targeted ES cells were injected into B6(Cg)-*Tyr*$^{c-2j}$ blastocysts. Chimera were bred to B6(Cg)-*Tyr*$^{c-2j}$ mice (JAX No. 0058) to achieve germ line transmission. Mice carrying the targeted mutation (*Grin1* floxed Neo) were bred to the germ line cre strain B6-Tg (Zp3-cre) (JAX No. 3651) to generate the *Grin1*ΔEx5 allele. Genotyping was performed using three primers: 5'-AGCTCACCCTCACTTGTAACCACA-3', 5'-ATGCAAGGGCAGGCAGTATAGTCT-3', and 5'-GCTGAAATGGACGGAGACTTAG-3', which amplify 91-bp and 260-bp products for wild type and mutant allele, respectively. The genotyping protocol has been validated using quantitative RT-PCR.

Reverse transcription (RT) and RT-qPCR. B6 mice aged P7 or P14 were anesthetized and decapitated and their brains were quickly removed. The ventral basal thalamus was dissected from coronal section of 1-mm thick, and quickly frozen in liquid nitrogen. The entire dissection process was done on ice using instruments treated with RNase Zap (Ambion). Total RNA was isolated using RNeasy Lipid Tissue Mini Kit (Qiagen). cDNA was synthesized from 2.0 μg of total RNA using High-Capacity cDNA Reverse Transcription kit (Applied Biosystems). Quantitative PCR (RT-qPCR) was performed with 15 ng of cDNA using SYBR GreenER^{TM} qPCR Master Mix (Invitrogen, Carlsbad, CA, USA) in an ABI Prism 7000 Sequence Detection System (Applied Biosystems). The primers for RT-qPCR were in Table S1. For each of these genes, the primers span intron/exon boundaries. All reactions were run in triplicate, and the specificity of the reactions was determined by analyzing the melting curves. Expression levels were normalized to the housekeeping gene *Pgk1*.

Table S1. Primer sequences for RT-qPCR.

Transcript	Forward primer	Reverse primer
Grin1 (total)	AGCAAAATGTGTCCCTGTCC	GCATCCTTGTGTCGCTTGTA
Grin1 with exon 5	AGAAGCGCCTGGAGACGTTG	CGCGCTTGTTGTCATAGGACAGTT
Grin1-1	TGGCCTCCAGCTTCAAGAGACGTA	TCGCGGCAGCACTGTGTCTTT
Grin1-2	AACGTGTGGAGGAAGAACCT	TCCTCCCTCTCAATAGCGCGT
Grin1-3	AGAGACGTAGGTCCTCCAAAGACA	TGACCGAGGGATCTGAGAGGTTGA
Grin1-4	AACGTGTGGAGGAAGAACCT	TCACACCACGGTGCTGACCGA
Grin2a	TCACTGAGGAAGGCTATCAGGT	GGCTCACAGTCAGAAAAGGACT
Grin2b	AACGGTCAGAGGTGGTTGAC	AGCAGAGACAATGAGCAGCA
Pgk1	CTCCGCTTTCATGTAGAGGAAG	GACATCTCCTAGTTTGGACAGTG

Slice electrophysiology. Brain slices were prepared using methods described previously (2). Briefly, mice were anesthetized and decapitated. Brains were quickly removed and placed in ice-cold solution containing (in mM): 210 Sucrose, 3.0 KCl, 1.0 $CaCl_2$, 4.0 $MgSO_4$, 1.0 NaH_2PO_4, 26 $NaHCO_3$, 10 glucose, saturated with 95% O_2 and 5% CO_2. Sagittal and coronal slices were prepared for thalamic and cortical recordings, respectively. Slices were cut at 300 μm on a vibrating tissue slicer (VT 1200, Leica, Germany) and kept in artificial cerebral spinal fluid (ACSF) containing (in mM): 124 NaCl, 3.0 KCl, 1.5 $CaCl_2$, 1.3 $MgCl_2$, 1.0 NaH_2PO_4, 26 $NaHCO_3$, and 20 glucose, saturated with 95% O_2 and 5% CO_2 at room temperature (21-23 °C). Slices were allowed to recover for at least one hour before recording.

For recording, a slice was transferred to submerge-type chamber where it is continuously exposed to ASCF at 32-33 °C saturated with 95% O_2 and 5% CO_2 and flowing at the speed of 2.2 ± 0.2 ml/min. For thalamic recordings, whole-cell patch clamp recordings were made from the soma of VPm neuron using a Multiclamp 700B amplifier (Molecular Devices, Sunnyvale, CA, USA). The pipette solution contained (in mM): 110 Cs methylsulfate, 20 TEA-Cl, 15 CsCl, 4 ATP-Mg, 0.3 GTP, 0.5 EGTA, 10 HEPES, 4.0 QX-314 and 1.0 spermine (pH 7.2, 270-280 mmol kg^{-1} with sucrose). Electrodes had resistances between 2 and 4 MΩ. The series resistance (R_s), usually between 7 to 12 MΩ, was not compensated. Data was discarded when R_s was > 18 MΩ. A concentric bipolar electrode (FHC, Bowdoin, ME, USA) was placed in the medial lemniscus to stimulate axons from the Pr5, and current pulses (100 – 400 μA, 200 μs in duration) were applied at 0.1 Hz. For evoked EPSCs in cortical neurons, whole-cell recordings were made from the soma of layer 5 pyramidal neurons. Stimulation electrodes were made of twisted nichrome microwires (38 μm in diameter with coating, A-M Systems) and placed in the layer 5 about 300 μm away from the recorded neurons. GABAergic transmission was blocked by picrotoxin (100 μM). AMPAR-EPSCs were blocked by DNQX (10 μM).

Quantal synaptic events were recorded without synaptic blockers but in the presence of tetrodotoxin (TTX, 0.3 μM). The pipette solution contained (in mM): 110 Cs methylsulfate, 10 CsCl, 4 ATP-Mg, 0.3 GTP, 0.5 EGTA, and 10 HEPES (pH 7.2, 270-280 mmol kg^{-1} with sucrose). Under this condition, the reversal potential of Cl^- was -65 mV. Excitatory miniature synaptic currents (mEPSCs) were recorded at -65 mV, and inhibitory miniature synaptic currents were recorded at 0 mV.

Recordings were conducted using AxoGraph X (AxoGraph Scientific, Sydney, Australia). Data were filtered at 4 kHz and digitized at 20 kHz. QX-314, picrotoxin and TTX were obtained from Tocris (Ellisville, Missouri USA), and all other chemicals were from Sigma-Aldrich (St. Louis, MO USA).

Nucleated patch recording. Nucleated patch recording was performed as described previously (3). After achieving whole-cell configuration, negative pressure (90-100 mmHg) was applied to the recording pipette while it was slowly pulled away from the cell. Using this procedure, large patches of membrane engulfing the cell nucleus could be obtained for recording. Pressure was reduced to 50-60 mmHg during recording. For fast agonist application, solutions were applied by gravity feed through theta glass pipettes with a tip diameter of about 200 μm. The theta pipettes were mounted on a piezoelectric transducer and fast switching was controlled using a piezo driver (E-650, Physik Instrumente, Karlsruhe, Germany) and a voltage ramp protocol. The speed of solution exchange was measured in the end of each experiment by measuring junction potential change with an open electrode when switching from ACSF to 30% ACSF.

Analysis of electrophysiological data. All data analyses were done using AxoGraph X. NMDAR-EPSC decay constant was measured from EPSCs recorded at +40 mV. The decay phase of NMDAR-EPSCs was best fitted by the double exponential function:

$$I = A_1 e^{-t/\tau 1} + A_2 e^{-t/\tau 2}$$

where A_1 and A_2 are the maximum amplitudes of the fast and slow components, and τ_1 and τ_2 are the decay time constants of the two components. A 600-ms segment starting from the peak of EPSCs was used for exponential fit. The weighted decay time constant τ_w was calculated as:

$$\tau_w = (A_1 \tau_1 + A_2 \tau_2) / (A_1 + A_2).$$

The AMPAR/NMDAR ratio was estimated by recording EPSC at -70 mV and +40 mV at the same stimulus intensity from the same cell. The peak amplitude at -70 mV was used for AMPAR-EPSC. For NMDAR-EPSC at +40 mV, amplitude at 10 ms after the beginning of EPSCs was measured.

For quantal event analysis, data were filtered at 1 kHz, and events were detected using variable-amplitude templates as described previously (4). For each neuron 200 to 800 events were analyzed and averaged.

Labeling and imaging of dendritic spines. Neurons were labeled during whole-cell recording for 10 minutes with 0.3% biocytin included in the patch pipette. Slices were fixed in 4% paraformaldehyde at 4 °C for at least 24 hrs. After wash, slices were incubated with DyLight 594 streptavidin (1:500, SA-5549, Vector Laboratories, Burlingame, CA) at 4 °C for 24 hrs. Slices were mounted in Prolong Gold (Invitrogen). Imaging and analysis were performed with experimenter blind to genotype. Confocal stacks were imaged with 63x objective (NA 1.4) and a 5x optical zoom on Leica SP5 confocal microscope. The pixel size was 96 nm and the z-step size was 130 nm. For basal dendrites, 4 or 5 segments at least 100 μm away from the soma were imaged. For apical dendrites, 4 or 5 segments located in layer 2/3 were imaged. Data were analyzed using ImageJ. Confocal stacks were z-projected at the maximal intensity. The number of dendritic spines was counted manually using the Multi-point Tool and the length of dendritic segment was measured with the Segmented Line Tool in ImageJ.

Seizure induction. Pentylenetetrazole (PTZ, Sigma, P6500) was dissolved in 0.9% saline at 5.0 mg/ml and administrated to adult mice of 4-7 months of age by intraperitoneal injection. Each mouse received a single injection and the dose was 50 mg/kg for male and 40 mg/kg for female mice. Kainic acid (KA, abcam, ab120100) was dissolved in 0.9% saline at 3.0 mg/ml, and administrated at 15 mg/kg to adult male mice of 3-7 months of age by intraperitoneal injection. Mutant and control mice were either littermates or age matched. Experiments and analyses were performed with experimenter blind to genotype.

For PTZ-induced seizures, mice were recorded for 30 min after the injection with a digital camera and analyses were performed post hoc. Myoclonic jerk is defined as jerking movement of the neck associated with tail clonus. Generalized tonic-clonic seizure is defined as complete loss of postural control associated with tonic-clonic movement of forelimb and hind limb.

For KA-induced seizures, mice were recorded for 100 min after the injection. Clonic seizure is defined as repeated jerking of limbs and loss of posture. Status epilepticus is defined repeated seizure activity (two or more clonic or tonic-clonic seizures within a 5-minute window) that lasts for 15 minutes or longer.

TUNEL assay and immunostaining. Two days after KA injection, mice were perfused with 4% paraformaldehyde and post fixed at 4 °C over night. Sagittal brain sections were cut at 60 μm in thickness. TUNEL assay was performed using the HRP-DAB kit (ab206386, abcam). Immunostaining was performed using antibodies for cleaved caspase 3 (rabbit, 1:200, Cell Signaling, #9509) and NeuN (mouse, 1:1000, Millipore, MAB377).

Statistics. Statistics was performed using GraphPad Prism (GraphPad Software, San Diego, CA) and JMP (SAS, Cary, NC). Throughout, means are given ± SEM. Unless specified otherwise, means were compared using Mann-Whitney test (between two groups), or Kruskal-Wallis test (between three or more groups).

Reference

1. Kadotani H, Hirano T, Masugi M, Nakamura K, Nakao K, Katsuki M, et al. Motor discoordination results from combined gene disruption of the NMDA receptor NR2A and NR2C subunits, but not from single disruption of the NR2A or NR2C subunit. J Neurosci. 1996;16(24):7859-67.
2. Arsenault D, Zhang Z W. Developmental remodelling of the lemniscal synapse in the ventral basal thalamus of the mouse. J Physiol. 2006;573(Pt 1):121-32.
3. Sather W, Dieudonne S, Macdonald J F, Ascher P. Activation and desensitization of N-methyl-D-aspartate receptors in nucleated outside-out patches from mouse neurones. J Physiol. 1992;450:643-72.
4. Zhang W, Peterson M, Beyer B, Frankel W N, Zhang Z W. Loss of MeCP2 from forebrain excitatory neurons leads to cortical hyperexcitation and seizures. J Neurosci. 2014;34(7):2754-63.

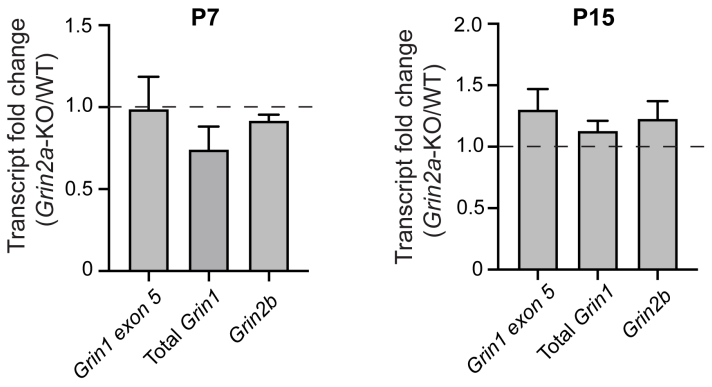

Figure S1. Deletion of *Grin2a* had no effect on the expression of exon-5-containing *Grin1* or *Grin2b* in the thalamus. Quantitative RT-qPCR was performed on thalamic tissues dissected from *Grin2a*-KO and WT mice at P7 (left panel) and P15 (right panel). There was no difference in the number of transcripts for exon-5-containing *Grin1*, total *Grin1*, or *Grin2b* between *Grin2a*-KO and WT at P7 or P15 ($p > 0.05$, t-Test).

Figure S2. Conserved DNA sequence alignment of *Grin1* exon 5. DNA sequences were obtained from *Ensembl*. Alignment was performed using the multiple sequence alignment tool T-Coffee (https://www.ebi.ac.uk/Tools/msa/tcoffee/). Stars (*) indicate conserved nucleotides. Non-conserved nucleotides were underlined. DNA sequences of *Grin1* exon 5 are 100% identical between human, macaque, and mouse, 97% identical between human and chicken, 95% identical between human and Xenopus, and 90% identical between human and zebrafish.

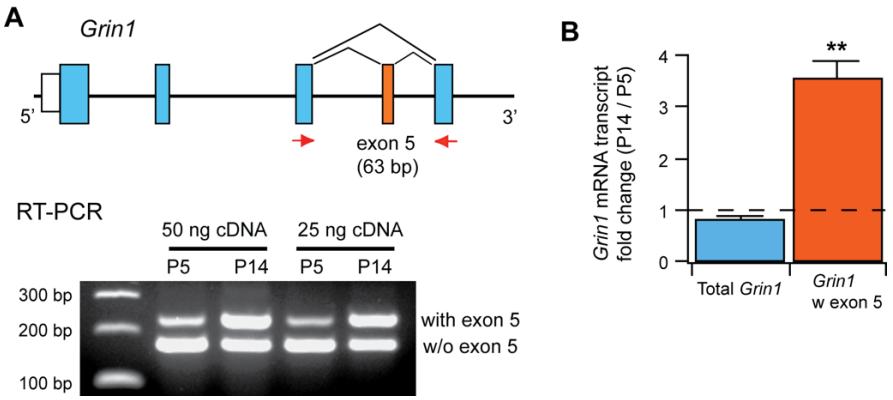

Figure S3. Upregulation of exon-5-containing *Grin1* transcripts in the thalamus of the mouse during early life. (**A**) Upper panel: a schematic view of the 5' region of *Grin1* with exon 5 highlighted in orange. The locations of RT-PCR primers are indicated by the arrows in red. Lower panel shows RT-PCR results of thalamic tissues at P5 and P14 using 50 and 25 ng cDNA as template. The upper band indicates *Grin1* transcripts with exon 5. (**B**) Fold changes in *Grin1* transcripts in the thalamus between P5 and P14 measured by RT-qPCR. Data were obtained from 5 mice each at P5 and P14. **p = 0.005 (total vs. exon-5-containing transcript), t Test, DF = 4.33, t = 7.79.

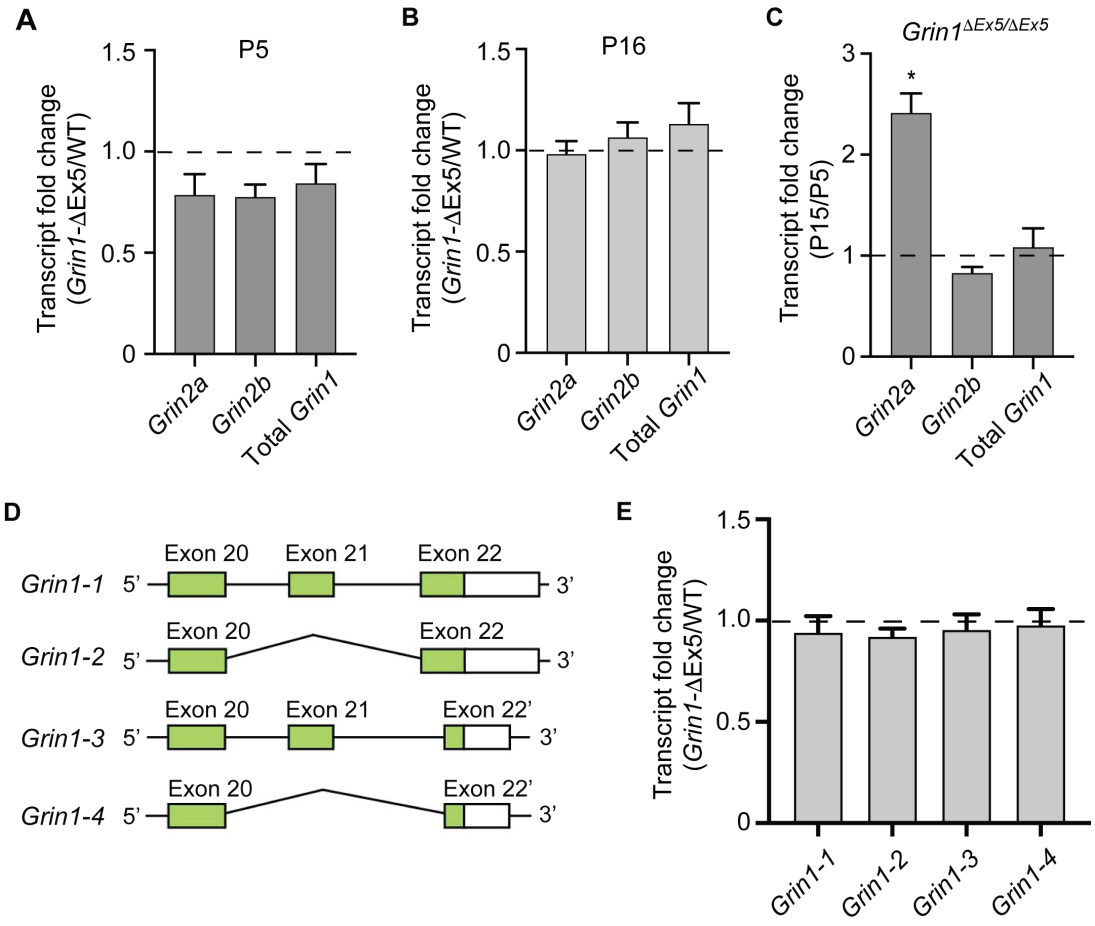

Figure S4. Deletion of *Grin1* exon 5 did not alter the up-regulation of GluN2A in the thalamus or the expression of GluN1 C-terminal variants. (A) Results of RT-qPCR using thalamic tissues dissected from *Grin1*$^{\Delta Ex5/\Delta Ex5}$ (n = 3) and WT (n = 3) mice at P5. There was no difference between mutant and WT in *Grin2a*, *Grin2b*, total *Grin1* ($p > 0.05$, t-Test). (**B**) Results of RT-qPCR at P16 from *Grin1*$^{\Delta Ex5/\Delta Ex5}$ (n = 4) and WT mice. There was no difference between mutant and WT in *Grin2a*, *Grin2b*, total *Grin1* ($p > 0.05$, t-Test). **(C)** Results of RT-qPCR using thalamic tissues dissected from *Grin1*$^{\Delta Ex5/\Delta Ex5}$ mice at P5 (n = 3) and P15 (n = 3). The number of *Grin2a* transcripts doubled between P15 and P5 ($p = 0.018$, t-Test, $t = 7.36$, $df = 2$), whereas those of *Grin2b* or total *Grin1* were unchanged ($p > 0.05$, t-Test). (**D**) Schematic view of GluN1 C-terminal variants. (**E**) Results of RT-qPCR using thalamic tissues dissected from *Grin1*$^{\Delta Ex5/\Delta Ex5}$ (n = 3) and WT (n = 3) mice at P16. There was no difference between mutant and WT in any of the transcripts ($p > 0.05$, t-Test).

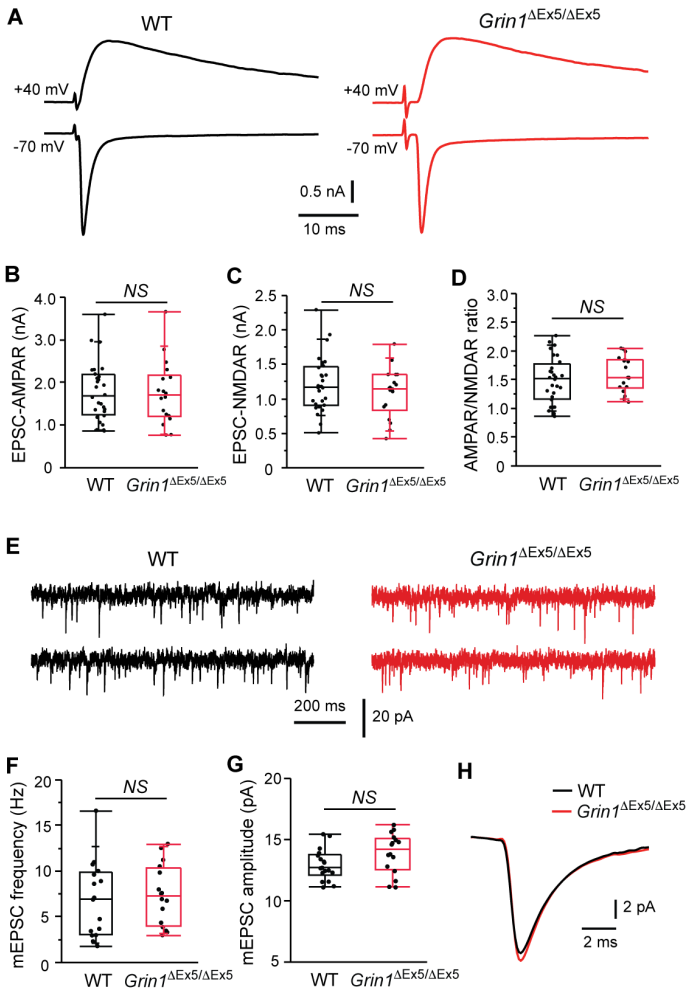

Figure S5. **Deletion of *Grin1* exon 5 has no effect on AMPAR function in thalamic neurons.** (**A**) Examples of AMPAR- and NMDAR-EPSCs recorded in a WT and a homozygous *Grin1*ΔEx5 neuron at P16. For each neuron, AMPAR- and NMDAR-EPSCs were recorded at the same stimulus intensity. (**B**), (**C**) and (D) Amplitudes of maximal AMPAR- and NMDAR-EPSCs, and AMPAR/NMDAR ratio of WT (n = 28 cells from 5 mice) and homozygous *Grin1*ΔEx5 neurons (n = 18 cells from 4 mice) at P16. The mean amplitude of AMPAR-EPSCs was 1779 ± 129 pA for WT and 1756 ± 174 pA for mutant (p = 0.84). The mean amplitude of NMDAR-EPSCs was 1216 ± 76 pA for WT and 1093 ± 84 pA for mutant (p = 0.47). The mean AMPAR/NMDAR ratio was 1.50 ± 0.08 for WT and 1.60 ± 0.07 for mutant (p = 0.39). (**E**) Examples of mEPSCs recorded in VPm neurons from WT and homozygous *Grin1*ΔEx5 mice at P16. (**F**) & (**G**) Frequency and amplitude of mEPSCs recorded in WT (n = 18 cells from 3 mice) and mutant (n = 16 cells from 3 mice) VPm neurons. The mean frequency of mEPSCs was 6.97 ± 1.03 Hz for WT and 7.37 ± 0.83 Hz for mutant (p = 0.56). The mean peak amplitude of mEPSCs was 12.9 ± 0.3 pA for WT and 13.9 ± 0.4 pA for mutant (p = 0.07). (**H**) Averaged mEPSCs from WT (black) and homozygous *Grin1*ΔEx5 neurons at P16. The mean rise time of mEPSC was 0.49 ± 0.02 ms for WT, and 0.47 ± 0.02 ms for mutant (p = 0.57). The mean decay constant of mEPSC was 2.28 ± 0.12 ms for WT and 2.28 ± 0.12 ms for mutant (p = 0.88).

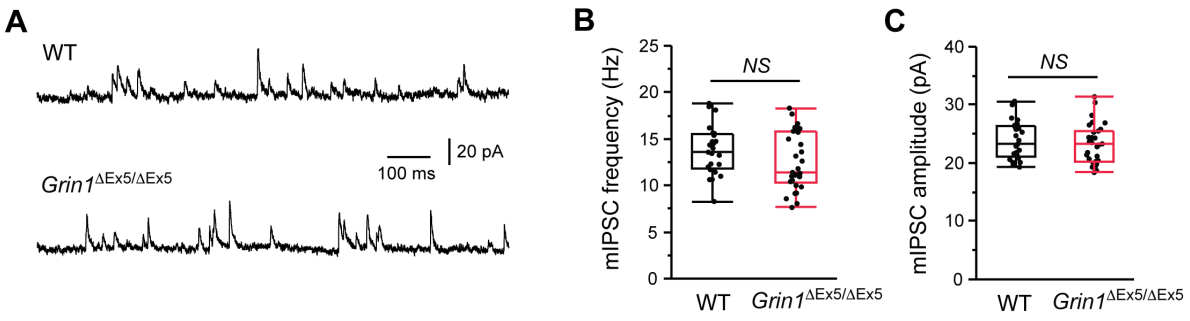

Figure S6. Deletion of *Grin1* exon 5 has no effect on quantal GABAergic synaptic currents in layer 5 pyramidal neurons. (**A**) Examples of mIPSCs recorded in layer 5 pyramidal neurons from WT and homozygous *Grin1*ΔEx5 mice at P17. (**B**) & (**C**) Frequency and amplitude of mIPSCs recorded in WT (n = 33 cells from 4 mice) and mutant neurons (n = 30 cells from 4 mice). The mean frequency of mIPSCs was 13.7 ± 0.5 Hz for WT and 12.5 ± 0.6 Hz for mutant neurons (p = 0.09). The mean peak amplitude of mIPSCs was 23.8 ± 0.7 pA for WT and 23.2 ± 0.6 pA for mutant neurons (p = 0.43). The mean rise time of mIPSC was 0.81 ± 0.02 ms for WT, and 0.86 ± 0.03 ms for mutant neurons (p = 0.42). The mean decay constant of mIPSC was 5.57 ± 0.08 ms for WT and 5.89 ± 0.14 ms for mutant neurons (*p* = 0.18).

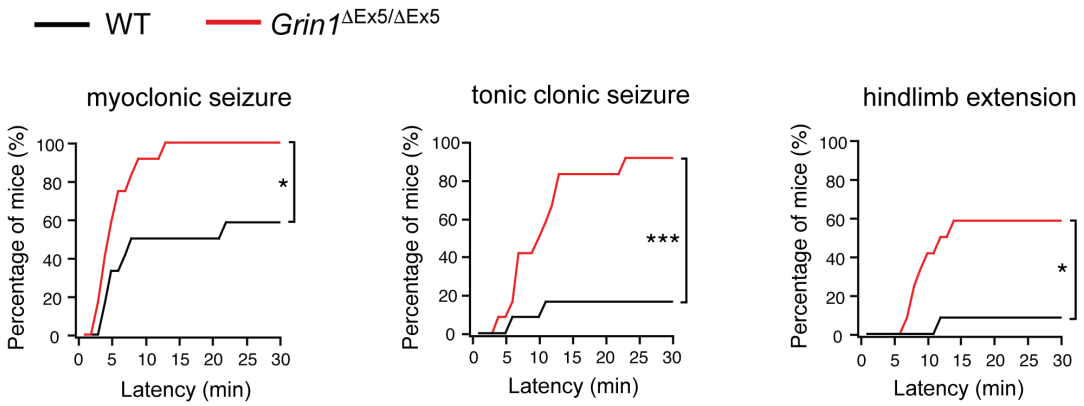

Figure S7. Deletion of *Grin1* exon 5 increases seizure susceptibility in adult female mice. A single dose of PTZ (40 mg/kg, i.p.) was administrated and the latency to the first episode of myoclonic jerk, generalized tonic-clonic seizure, and generalized tonic-clonic seizure with hindlimb extension was recorded. Data were obtained from 12 WT and 12 homozygous *Grin1*ΔEx5 mice. * $p < 0.05$; *** $p < 0.001$, two-tailed p values, Fisher's Exact Test.

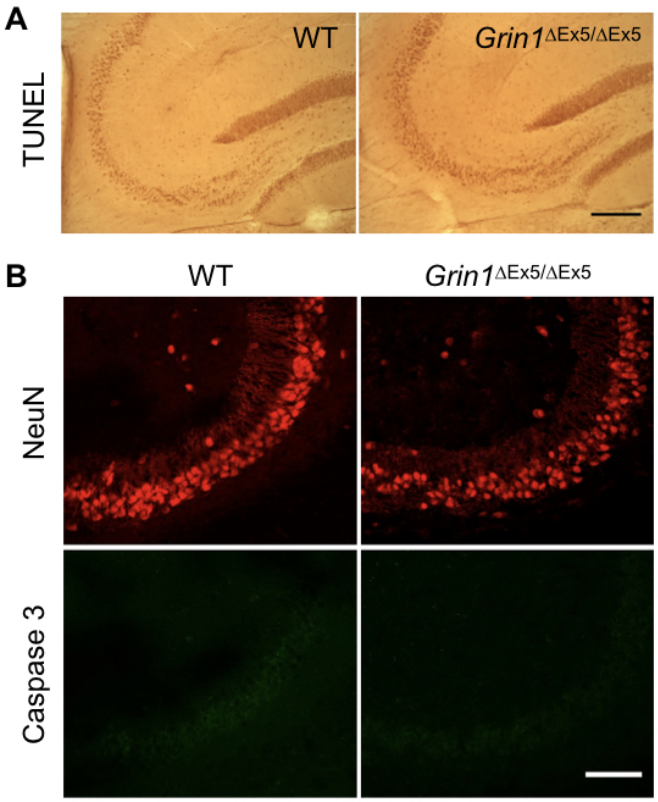

Figure S8. Lack of cell death in the brains of KA-injected mice. (A) Images of the hippocampal sections processed by TUNEL assay from WT and homozygous *Grin1*ΔEx5 mice two days after KA injection. Only background staining was observed in either brain. The mutant but not WT mouse showed status epilepticus in response to KA injection. Scale bar: 200 μm. (**B**) Confocal images of CA3 neurons in WT and homozygous *Grin1*ΔEx5 mice staining for NeuN and cleaved caspase 3. Scale bar: 100 μm.